

Estimating Summer Precipitation Over the Tibetan Plateau With Geostatistics and Remote Sensing

Author(s): Shi-Guang Xu , Zheng Niu , Da Kuang , Yan Shen , Wen-Jiang Huang , and Yu Wang

Source: Mountain Research and Development, 33(4):424-436. 2013.

Published By: International Mountain Society

DOI: <http://dx.doi.org/10.1659/MRD-JOURNAL-D-13-00033.1>

URL: <http://www.bioone.org/doi/full/10.1659/MRD-JOURNAL-D-13-00033.1>

BioOne (www.bioone.org) is a nonprofit, online aggregation of core research in the biological, ecological, and environmental sciences. BioOne provides a sustainable online platform for over 170 journals and books published by nonprofit societies, associations, museums, institutions, and presses.

Your use of this PDF, the BioOne Web site, and all posted and associated content indicates your acceptance of BioOne's Terms of Use, available at www.bioone.org/page/terms_of_use.

Usage of BioOne content is strictly limited to personal, educational, and non-commercial use. Commercial inquiries or rights and permissions requests should be directed to the individual publisher as copyright holder.

Estimating Summer Precipitation Over the Tibetan Plateau With Geostatistics and Remote Sensing

Shi-Guang Xu¹, Zheng Niu^{1*}, Da Kuang², Yan Shen³, Wen-Jiang Huang⁴, and Yu Wang⁵

* Corresponding author: niuz@irsa.ac.cn

¹The State Key Laboratory of Remote Sensing Science, Laboratory of Digital Earth Sciences, Institute of Remote Sensing and Digital Earth, Chinese Academy of Sciences, Beijing 100101, China

²Institute of Tibetan Plateau Atmospheric & Environmental Science, Lhasa, 85000, China

³National Meteorological Information Center (NMIC), China Meteorological Administration (CMA), 100081, Beijing, China

⁴Laboratory of Digital Earth Sciences, Institute of Remote Sensing and Digital Earth, Chinese Academy of Sciences, Beijing 100094, China

⁵China University of Geosciences, Beijing School of Land Science Technology, Beijing, China

Open access article: please credit the authors and the full source.



Although precipitation is important to climatology, hydrology, and agricultural research, the spatial pattern of precipitation over the Tibetan Plateau is difficult to determine because of complex surface conditions and a sparse rain gauge

network. In the present article, a method we named *FETCH_OCK*—based on a combination of Yin et al's Fetch method (2008) and ordinary cokriging (*OCK*)—is proposed; it was used to estimate monthly summer precipitation over the Tibetan Plateau, which has limited rain gauge observations and a restricted satellite precipitation dataset. First, the monthly ground observations measured by rain gauges were interpolated using *OCK*, with a digital elevation model (*DEM*) as the covariant. Second, the spatial variability of the precipitation monitored by satellite was extracted from the Climate Prediction Center morphing (*CMORPH*) satellite precipitation dataset by calculating a parameter (*FETCH*)

developed from Yin et al's Fetch parameter. Finally, the precipitation datasets estimated by *OCK* were corrected by the *FETCH* parameter derived from the *CMORPH* satellite precipitation dataset. Summer (June to August) precipitation over the Tibetan Plateau from 2005 to 2009 was estimated using this model. The precipitation datasets estimated by *FETCH_OCK* were tested using ground observations from 55 independent rain gauges. The results indicate that the *FETCH_OCK* model not only is an improvement compared with the input precipitation datasets (*OCK* and *CMORPH*) but also performs better than other widely used precipitation datasets, including universal kriging with *DEM* as a covariant and Tropical Rainfall Measuring Mission 3B43. The present study aims to correct the smoothing effect of kriging interpolation models and to provide a more accurate precipitation dataset for the Tibetan Plateau.

Keywords: Precipitation; cokriging; digital elevation model (*DEM*); Climate Prediction Center morphing (*CMORPH*); data fusion; *FETCH_OCK*; Tibetan Plateau.

Peer-reviewed: July 2013 **Accepted:** September 2013

Introduction

The Tibetan Plateau is the highest region in the world, with elevations generally higher than 4000 m above mean sea level. This region is an important source of several major rivers, such as the Yangtze, Yellow, Lancang–Mekong, Salween–Nujiang, Ganges–Brahmaputra, and Indus, so the precipitation over this region is of critical importance to the environment and livelihood of millions of people along these rivers (Yin et al 2008; Li and Shao 2010; Wu and Chen 2012). Therefore, it is important to obtain accurate precipitation data over this region to understand the spatial and temporal variation characteristics of precipitation.

A rain gauge can provide accurate precipitation data at the gauge location, but the rain gauge network on the Tibetan Plateau is still sparse because of natural

conditions and high elevation, making it difficult to estimate the precipitation over this region. Various methods have been developed to analyze the spatial pattern of precipitation with ground observations measured by rain gauges (Villarini and Krajewski 2008; Michaelides et al 2009; Ward et al 2011), and extensive research has shown that geostatistical interpolation based on geographical information systems can provide more accurate precipitation estimates than other interpolation or regression models (Lloyd 2005; Bostan et al 2012). In geostatistical interpolation models, the precipitation over ungauged areas is interpolated from nearby samples and a semivariogram is calculated by the semivariance of each point pair (Goovaerts 1998; Diodato et al 2010; Kebaili Bargaoui and Chebbi 2009). In recent decades, the thermal and dynamic forcing mechanisms of topography on the atmospheric circulation and precipitation

distribution have been widely discussed, and elevation has been reported to have potential to improve the accuracy of geostatistical models when integrated into the interpolation process (Sokol and Bližňák 2009; Um et al 2011). Goovaerts (2000) and Lloyd (2005) established several multivariate geostatistical interpolation models by integrating elevation into the kriging model, including cokriging, kriging with an external drift, simple kriging with a locally varying mean, and ordinary cokriging (OCK). Their research showed that when elevation is closely related to precipitation, the precision of the kriging model can evidently be improved. But these gauge-based analyses largely depend on the density and configuration of the rain gauge network, so for undeveloped or remote areas with a sparse rain gauge network, these methods are insufficient to estimate the spatial pattern of precipitation (Xie and Xiong 2011).

Another reliable method for acquiring precipitation data is reproducing the physics of precipitation formation. A number of physical models based on parameterization of microphysics have been established to estimate and predict precipitation by considering the microphysical processes of precipitation, temperature, and humidity and the effects of clouds on condensation and evaporation (Tripoli and Cotton 1980; Zhao and Carr 1997; Rotstajn 1998). But the application of such methods would make a set of model equations too complicated, and many necessary datasets are hard to obtain (Akimov 2004). With the development of meteorological satellite networks, information from spaceborne sensors has greatly expanded the coverage of ground observation and provides an effective approach to monitoring the precipitation over remote areas. Satellite precipitation datasets are derived from brightness temperature observed by infrared, microwave, or both types of sensors using statistical or physical retrieval algorithms. The visible and infrared satellite data can monitor the temperature on the tops of clouds (Arkin and Meisner 1987; Brown 2006; Haile et al 2010), while the microwave observations can reflect the thermal emission of raindrops at low frequency (10–37 GHz) and the scattering of upwelling radiation from Earth into space (85 GHz and higher) (Ferraro 1997; Grody 1984; Kidd and Levizzani 2011).

Based on these discoveries, a number of satellite-driven precipitation models have been established with the infrared and microwave data. Arkin and Meisner (1987) estimated the precipitation with infrared satellite observation. Grody (1991) proposed the scatter index method based on the differences in the scattering effect of the hydrometeors for different microwave channels. Furthermore, a series of studies has been conducted to merge the information from infrared and microwave satellite observations to provide precipitation data with high spatial and temporal resolution (Xie and Arkin 1996, 1997; Grimes et al 1999; Gruber et al 2000).

However, the relationship between cloud physical variables and precipitation varies in different areas, so the precipitation datasets derived from satellite observations usually contain varying regional biases and random errors, which limits the use of satellite precipitation data in many scientific applications (Turlapaty et al 2010; Xie and Xiong 2011), especially in mountainous areas with complicated underlying surfaces (Ward et al 2011).

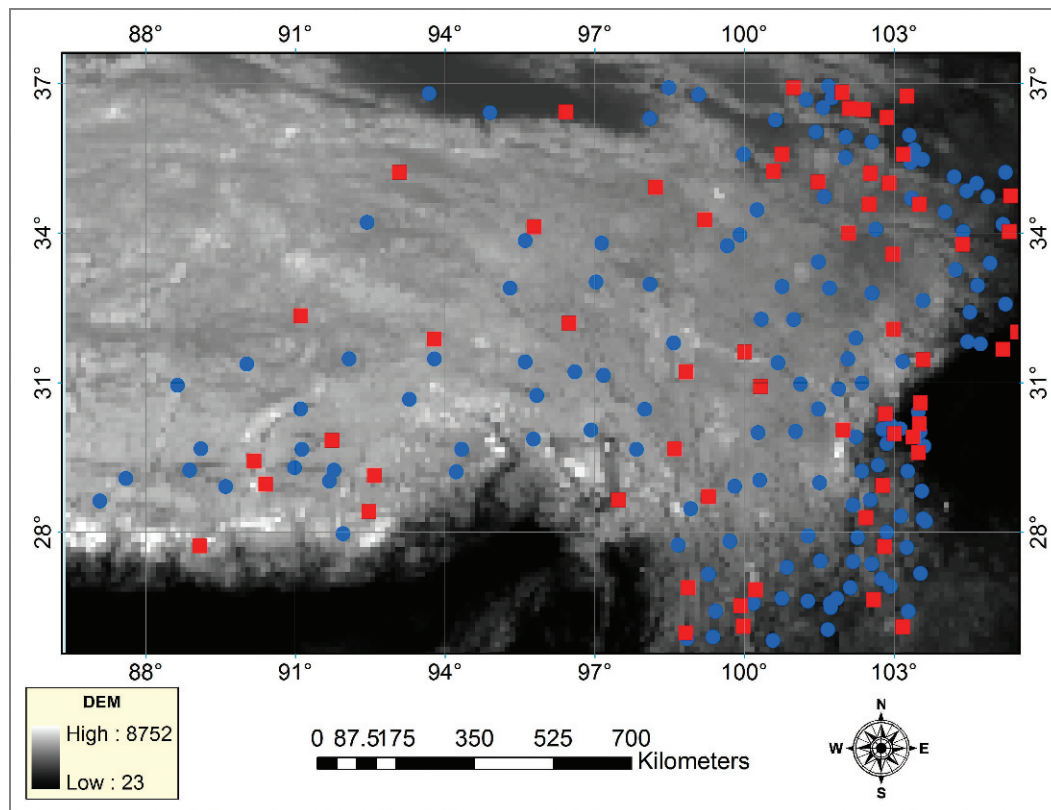
As part of the project conducted by the China Meteorological Administration to provide an accurate precipitation dataset over the Tibetan Plateau, this study developed a new model to estimate the precipitation over the Tibetan Plateau with limited rain gauge observations and a satellite precipitation dataset. We named this model FETCH_OCK, because it combines a method we call FETCH, based on Yin et al's Fetch method (2008), and OCK interpolation. Our FETCH_OCK model was established on the assumption that small-scale spatial variability in the precipitation monitored by satellites can improve the results of geostatistical interpolation, which are too smooth to present the complicated spatial pattern of precipitation over the Tibetan Plateau. The model was used to estimate the summer precipitation (June to August) between 2005 and 2009 over the Tibetan Plateau, with ground observations from 133 rain gauges and the monthly Climate Prediction Center morphing (CMORPH) satellite precipitation data as inputs. The results were validated using 55 rain gauge observations that were not included in the training. The performance of this new model was further assessed by comparing it with the precipitation datasets generated by universal kriging (UK) and the Tropical Rainfall Measuring Mission (TRMM) 3B43 multisource precipitation dataset.

Study area and materials

Study area

This study focused on the eastern Tibetan Plateau and the surrounding areas, with an area of approximately 1.1 million km², ranging from 25.5°N to 37.6°N and 86.4°E to 105.5°E (Figure 1). The special topography of the Tibetan Plateau results in a complicated climatic system that is different from that of surrounding areas. The eastern part of this region is affected by the East Asian monsoon, but the precipitation in the area is not very high because the moist airstream from the sea travels a long distance and is obstructed by the Hengduan Mountains. Another source of precipitation is the Indian monsoon from the Indian Ocean. Most of the moist airstream is obstructed and turned into large-scale precipitation by the Himalayas, but some of the air travels along the Brahmaputra and brings flush precipitation to the middle of the study area. The western region is drier because neither the East Asian monsoon nor the Indian

FIGURE 1 DEM of the study area and location of the 188 rain gauges used in this study.



monsoon can reach it. The temporal distribution of precipitation over the Tibetan Plateau shows apparent seasonal characteristics, with most precipitation coming between May and September (Shen et al 2011).

Data

Ground observation from rain gauges: The ground observations used in the study were measured with 188 rain gauges managed by the Institute of Tibetan Plateau Atmospheric and Environmental Science. The maximum, minimum, and mean values and the variance in the precipitation for each month are shown in Table 1. These rain gauges are located in the middle and eastern parts of the Tibetan Plateau with elevations ranging from 2437 to 4728 m (as shown in Figure 1). The number of rain gauges is too limited to accurately monitor the precipitation over this vast plateau, but the configuration of these rain gauges is relatively even. In this study, these rain gauge observations were separated into a training dataset and a testing dataset: 133 rain gauges (labeled as circles in Figure 1) were randomly selected, and the observations from these rain gauges were used to estimate the precipitation over the Tibetan Plateau with the FETCH_OCK model, while the observations from the remaining 55 rain gauges (labeled as rectangles in Figure 1) were used to assess the performance of the model in this study.

Satellite data: The satellite precipitation datasets used in this study included CMORPH and TRMM 3B43 V6. The former was used as the input for the FETCH_OCK model, while the latter was used as a comparison to assess the performance of this new model.

CMORPH is a multisatellite precipitation dataset produced by fusing the precipitation derived from infrared and microwave remote sensing data. The infrared-driven precipitation datasets with a half-hour temporal resolution from several satellites (Meteosat, the Geostationary Meteorological Satellite, etc) are used to estimate the motion vectors to propagate the 3-hour precipitation estimates derived from passive microwave data (Joyce et al 2004). A series of CMORPH precipitation datasets with various spatial and temporal resolutions have been developed and published to date. In this study, the 3-hour global microwave-based precipitation with a $0.25^\circ \times 0.25^\circ$ spatial resolution contained in the CMORPH precipitation dataset was selected as the input for the FETCH_OCK model. To simulate the monthly precipitation over the Tibetan Plateau, the 3-hour CMORPH precipitation datasets were accumulated on a monthly timescale.

TRMM 3B43 V6 consists of monthly precipitation data generated by an algorithm whose aim is to produce the best estimate of precipitation rates (in millimeters per hour) and root-mean-square precipitation-error estimates based on

TABLE 1 Maximum (max) precipitation, minimum (min) precipitation, average (mean) precipitation, and variance of precipitation observed by 188 rain gauges between 2005 and 2009.

Year	Month	Max (mm)	Min (mm)	Mean (mm)	Variance
2005	Jun	303.5	3.8	99.89	63.80
	Jul	596.0	20.7	151.99	96.46
	Aug	440.4	4.3	144.49	86.36
2006	Jun	265.3	2.8	92.68	56.47
	Jul	428.2	14.7	123.83	77.06
	Aug	340.7	6.3	89.11	52.77
2007	Jun	312.1	6.3	97.85	49.79
	Jul	492.6	7.3	145.19	72.48
	Aug	740.5	5.8	135.88	104.58
2008	Jun	299.4	7.1	112.89	49.12
	Jul	492.8	1.3	137.07	77.79
	Aug	379.0	2.6	138.03	68.82
2009	Jun	341.1	0.0	97.97	68.46
	Jul	613.4	10.4	144.17	99.50
	Aug	473.8	2.4	129.89	62.10

multiple independent precipitation estimates from the TRMM Microwave Imager, Advanced Microwave Scanning Radiometer for Earth Observing Systems, Special Sensor Microwave Imager, Special Sensor Microwave Imager/Sounder, Advanced Microwave Sounding Unit, Microwave Humidity Sounder, microwave-adjusted merged geoinfrared, and monthly accumulated Global Precipitation Climatology Centre rain gauge analysis. These gridded precipitation datasets have a calendar-month temporal resolution and a $0.25^\circ \times 0.25^\circ$ spatial resolution (Condom et al 2011; Jia et al 2011; Karaseva et al 2012). In this study, the TRMM 3B43 V6 dataset covering the study area was downloaded from the National Aeronautics and Space Administration (2013). This dataset was used as a comparison to evaluate the performance of the FETCH_OCK model.

Digital elevation model data: The digital elevation model (DEM) data were obtained from the international scientific data service platform (Chinese Academy of Sciences, Computer Network Information Center, 2013). These data, measured by NASA and the National Imagery and Mapping Agency, contain a set of relative datasets, including slope, aspect, and topographic position index. In this study, the DEM was used as the covariance in the OCK interpolation. Because of the great extent of the study area, it was necessary to resample the DEM from $0.001^\circ \times 0.001^\circ$ to $0.1^\circ \times 0.1^\circ$ to reduce the computation load.

Methodology

OCK interpolation

OCK is a multivariate interpolation model derived from ordinary kriging (Li and Shao 2010). Apart from the sample data (rain gauge observation in this study), 1 or more types of relative spatial data such as DEM were also introduced into the interpolation process as auxiliary variables (also known as covariants). The covariants usually have a close relationship to the distribution of precipitation. Several studies have shown that OCK with DEM as a covariant can simulate more precisely than other spatial interpolation models. The cokriging precipitation estimating model with only 1 covariant according to Goovaerts (2000) is shown in Equation 1:

$$Z_{ck}(u) = \sum_{a=1}^{n(u)} l_a(u) Z(u_a) + l(u) [y(u) - m_y + m_z] \quad (1)$$

where $Z_{ck}(u)$ is the precipitation estimate result of cokriging at an unsampled location u ; $n(u)$ is the number of rain gauges used to simulate rainfall depth at location u ; $Z(u_a)$ is the value of the rain gauge observations at location u_a around location u ; $y(u)$ is the value of DEM at location u ; m_y and m_z are the global means of rain gauge observation and DEM, respectively; and $l_a(u)$ and $l(u)$ are the interpolation weights, which were calculated by solving Equation 2:

$$\begin{cases} \sum_{b=1}^{n(u)} l_b(u)g_{zz}(u_a - u_b) + l(u)g_{zy}(u_a - u) + m(u) = g_{zz}(u_a - u) \\ \sum_{b=1}^{n(u)} l_b(u)g_{zy}(u - u_b) + l(u)g_{yy}(0) + m(u) = g_{zy}(0) \\ \sum_{b=1}^{n(u)} l_b(u) + l(u) = 1 \end{cases} \quad (2)$$

where $l(u)$ and $m(u)$ are Lagrange parameters accounting for the constraints on the weights; $g_{zz}(h)$ and $g_{yy}(h)$ are the covariance functions of the rain gauge and DEM, respectively; and g_{zy} is the cross-semivariogram value between rain gauge observations and DEM.

The g_{zz} function is calculated by Equation 3:

$$g_{zz} = \left\{ \sum_{a=1}^h [z(u_a) - z(u_a + h)] \right\} / 2N(h) \quad (3)$$

where $z(u_a)$ is the rain gauge observation and $N(h)$ is the distance between each point pair.

The g_{yy} function is calculated by Equation 4:

$$g_{yy} = \left\{ \sum_{a=1}^h [y(u_a) - y(u_a + h)] \right\} / 2N(h) \quad (4)$$

where $y(u_a)$ is the value of elevation and $N(h)$ is the distance between each point pair.

The g_{zy} value is calculated by Equation 5:

$$g_{zy} = \left\{ \sum_{a=1}^{N(h)} [z(u_a) - z(u_a + h)][y(u_a) - y(u_a + h)] \right\} / 2N(h) \quad (5)$$

where $z(u_a)$ and $y(u_a)$ are the rain gauge observation and DEM, respectively.

In the interpolation process of OCK, self-correlation between the point data and the covariant was considered. Furthermore, the model considers cross-correlation between the covariant and the sample collection, which plays an important role in improving the precision of ordinary kriging. If the cross-correlation between the precipitation and the covariant is strong, the spatial continuity patterns between the precipitation and the covariant are similar, indicating that the covariant has a great influence on the interpolation. However, if there is low or no cross-correlation between the sample collection and the covariant, the effect of the covariant is negligible and OCK can be treated as ordinary kriging.

The FETCH_OCK model

Although OCK can derive unbiased estimates of regionalized variables at unsampled points from the values of the surrounding stations, this model has significant drawbacks when it is used to simulate the spatial pattern of precipitation over mountainous areas.

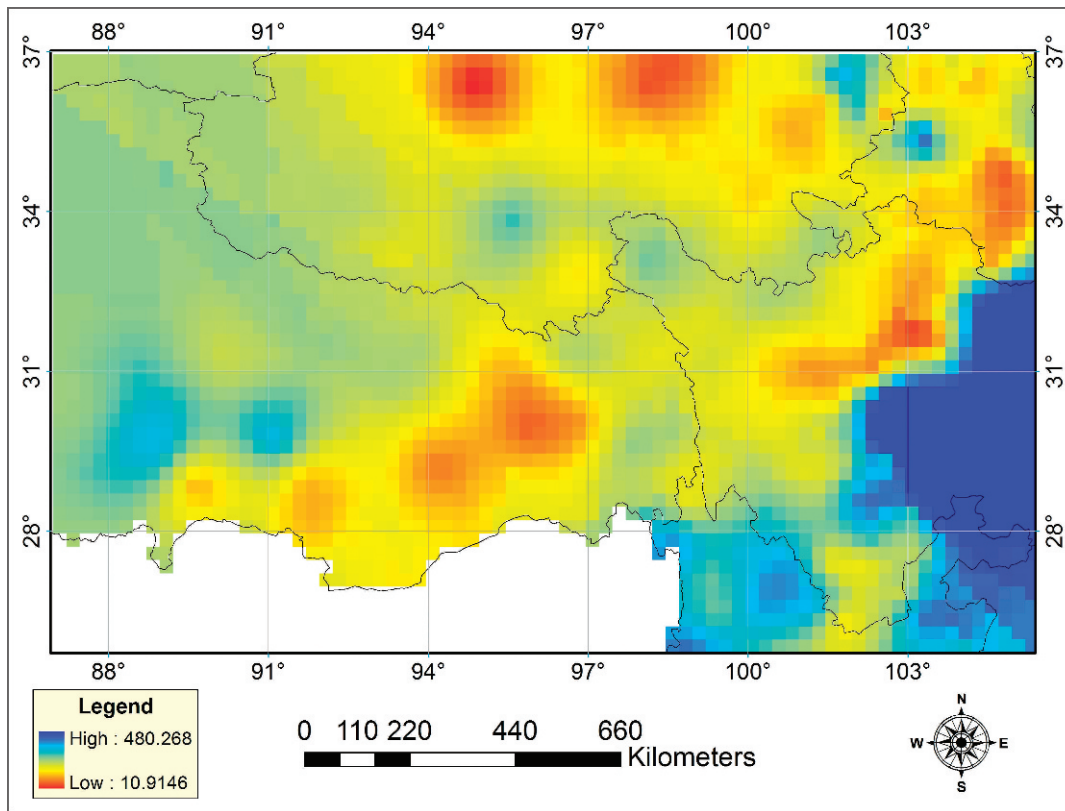
Precipitation is a complicated and discontinuous physical process affected by local atmospheric circulation, topographical local relief, land cover, and many other factors. These factors usually lead to obvious small-scale spatial variability in precipitation. Unfortunately, small-scale spatial variability of precipitation cannot be presented by OCK interpolation for 2 reasons. First, a dense and well-configured rain gauge network is essential to monitor the small-scale spatial variability of precipitation comprehensively, but the rain gauge network in remote and mountainous areas are usually sparse and located unevenly. Second, OCK fits the semivariogram with minimum mean-square-error-based methods, but all fitted curves generated by these methods are too smooth to present the extreme spatial variability given by the semivariogram. This shortcoming of OCK merits significant attention on the Tibetan Plateau, where the rain gauge network is sparse and the spatial pattern of precipitation is severely disturbed by the complicated underlying surface (Olea and Pawlowsky 1996; Yamamoto 2005).

Microwave remote sensing is a promising way to overcome the drawbacks of OCK. Compared with the limited coverage of the rain gauge network, the microwave meteorological satellites network can cover the whole Tibetan Plateau with high temporal resolution (3 hours). Another important advantage of microwave remote sensing is that microwave radiation can break through the clouds and provide the distribution of the precipitation particles, such as big raindrops and ice particles inside the clouds, so the microwave-based satellite precipitation datasets have a direct physical relationship with the real spatial pattern of precipitation. Based on the previous discussion, we assumed that the small-scale spatial variability of precipitation over the Tibetan Plateau can be observed by microwave remote sensing and reflected by the microwave-based satellite precipitation dataset. The FETCH_OCK model, which is aimed at correcting the smoothing effect of OCK and providing a more accurate precipitation dataset over the Tibetan Plateau, was established based on this assumption. Three steps are presented to describe the FETCH_OCK algorithm.

Step 1: The monthly precipitation measured by 133 rain gauges was interpolated by OCK, with DEM as a covariant, using Equations 1–5 and then resampled to $0.25^\circ \times 0.25^\circ$, which is the same as CMORPH. According to the semivariogram of rain gauges calculated by Equation 3, the semivariogram of DEM calculated by Equation 4, the cross-semivariogram between the rain gauge and DEM calculated by Equation 5, and the spherical model (Equation 6) were selected to fit each variogram (Goovaerts 2000). Equation 6 is as follows:

$$f(x) = \begin{cases} 1.5h/a - 0.5(h/a)^3, & a \geq h \\ 1, & a < h \end{cases} \quad (6)$$

FIGURE 2 Monthly precipitation (in millimeters) over the south Tibetan Plateau in August 2007 as calculated by the OCK interpolation with DEM as a covariant.



where a is the range of the variograms and h is the distance of the point data pairs.

Step 2: The small-scale spatial variability in the monthly CMORPH satellite precipitation dataset was extracted by calculating a parameter we named FETCH, because it was developed from the Fetch parameter proposed by Yin et al (2008). Yin et al's Fetch parameter is used to represent the spatial variability of an image; it is calculated by subtracting the smoothed image from the original image using a low-pass filter. In this study, Yin et al's Fetch parameter was modified by dividing their Fetch with the smoothed image to extract the spatial variability of CMORPH satellite precipitation datasets in the form of a ratio. This modified parameter was renamed FETCH.

The FETCH parameter was calculated using a 3-step algorithm. First, CMORPH was smoothed by a 3×3 moving window filter, which means the value of a grid in original image was substituted with the average value of the surrounding grids. Second, the smoothed CMORPH was subtracted from the original CMORPH. Finally, FETCH calculated with the result of step 2 was divided by the smoothed CMORPH. The algorithm was described by Equation 7:

$$FETCH(u) = \left[T(u) - \frac{\sum_{i=1}^8 T(i)}{8} \right] / T(u) \quad (7)$$

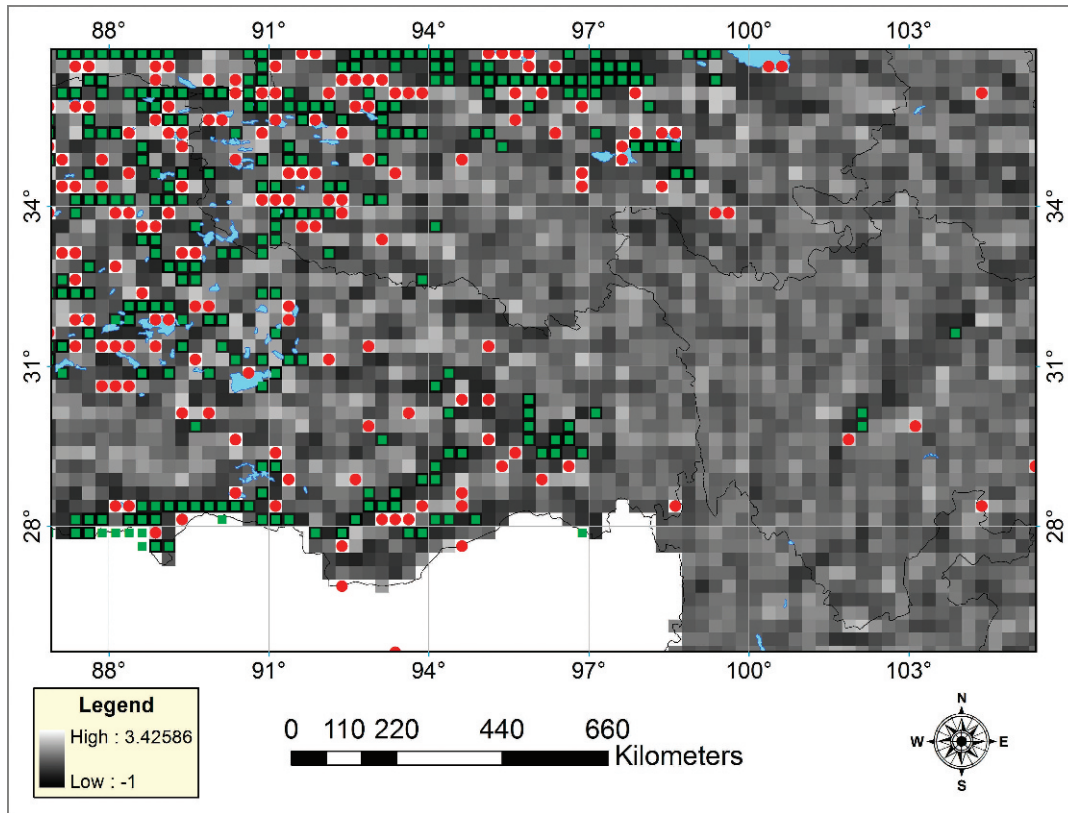
where $FETCH(u)$ is the value of FETCH in grid u , $T(u)$ is the value of CMORPH in grid u , and $T(i)$ is the value of the grids around grid u . The negative values of FETCH indicate that the precipitation of this grid in CMORPH is lower than that of the surrounding grids, and vice versa.

Step 3: The result of OCK (termed OCK_DEM) was corrected by FETCH following Equation 8. As shown in this equation, the grid in the result of OCK was multiplied by FETCH of the corresponding grids, and then the result was added to the original value of OCK.

$$FC(u) = FETCH(u) \times T_OCK(u) + T_OCK(u) \quad (8)$$

Here, $FC(u)$ is the result of FETCH_OCK in grid u , $FETCH(u)$ is the value of FETCH in grid u , and $T_OCK(u)$ is the result of OCK with DEM as a covariant.

FIGURE 3 Spatial distribution of FETCH in August 2007 on a 0.25° latitude–longitude grid. The circles represent the grid with FETCH below -0.2, while the rectangles represent the grid above 0.2.



Precision evaluation

The ground observations from 55 rain gauges that were not used in the training process were used to assess the performance of the models in the study. Four comparison criteria were calculated: mean absolute error (MAE), root-mean-square error (RMSE), coefficients of determination (R^2), and sum of squares of residuals (SSE). These criteria were calculated by Equations 9–12, respectively:

$$MAE = \sum_{k=1}^n |Y_k - O_k| / n \tag{9}$$

$$RMSE = \sqrt{\sum_{k=1}^n (Y_k - O_k)^2 / n} \tag{10}$$

$R^2 =$

$$\frac{\left\{ \sum_{k=1}^n [(Y_k - \bar{Y})(O_k - \bar{O})] \right\} / (n-1)}{\sqrt{\left[\sum_{k=1}^n (Y_k - \bar{Y})^2 \right] / (n-1)} \sqrt{\left[\sum_{k=1}^n (O_k - \bar{O})^2 \right] / (n-1)}} \tag{11}$$

$$SSE = \sum_{k=1}^n (Y_k - O_k)^2 \tag{12}$$

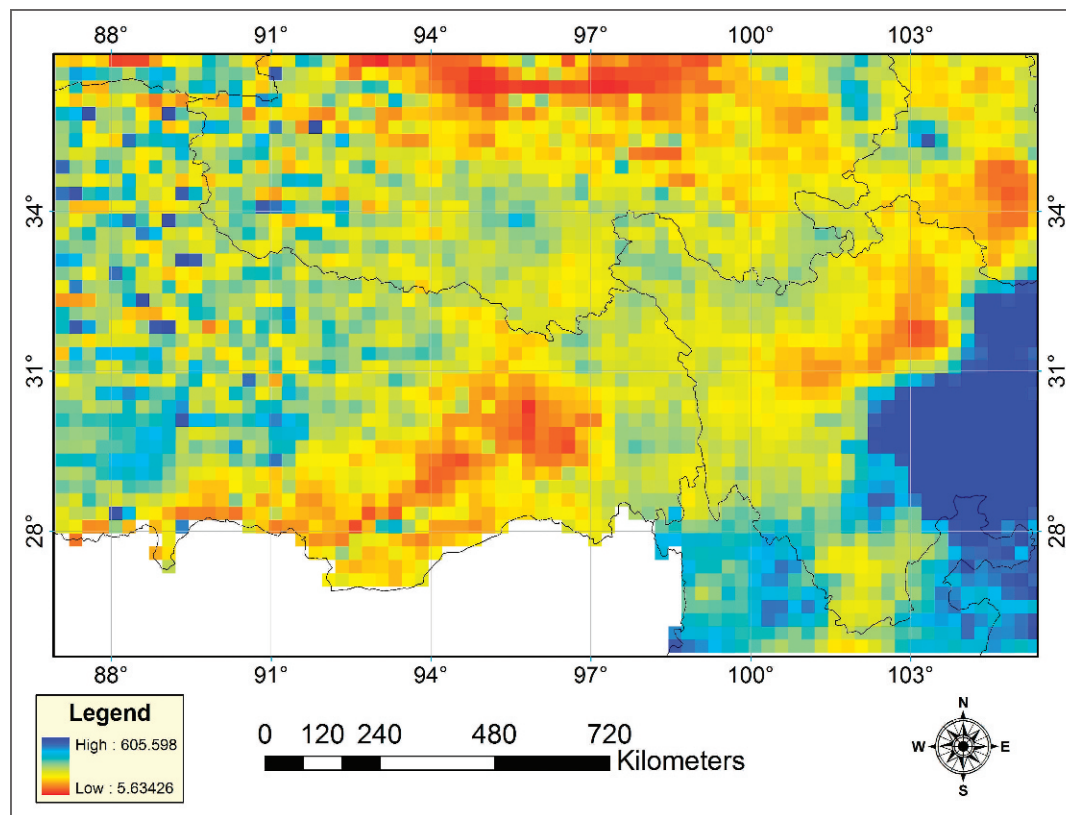
where Y_k is the observation measured by rain gauge k , O_k is the precipitation estimated by a model at the location of rain gauge k , \bar{Y} is the mean value of all rain gauge observations and the precipitation estimate value, and \bar{O} is the mean value of the precipitation at all rain gauge locations.

Results

The spatial pattern of OCK, FETCH, and FETCH_OCK

Figure 2 shows the precipitation dataset estimated by OCK, with DEM as a covariant (August 2007 is taken as an example). Although the complicated topography information was introduced into the interpolation process, the spatial distribution of precipitation estimated by OCK presented an evident smoothing effect. For example, in the Himalayas, where the Indian monsoon is seriously disturbed by the huge mountains, there should be a dramatic fluctuation between high and low precipitation on the southeast-facing and northwest-facing slopes for mountain ranges across the Tibetan

FIGURE 4 Monthly precipitation (in millimeters) dataset on a 0.25° latitude–longitude grid over the Tibetan Plateau in August 2007 as estimated by the FETCH_OCK model.



Plateau, according to the study by Yin et al (2008). But the spatial pattern of the precipitation estimated by OCK still presents a continuous surface, which cannot represent the thermal and dynamic forcing mechanisms of the topography.

Figure 3 presents the result of FETCH in August 2007, as derived from CMORPH satellite data. The circles and the rectangles in this figure represented grids with FETCH above 0.2 and below -0.2 , respectively. They indicated that the precipitation of CMORPH in these grids showed a distinct decrease (when FETCH was negative) or increase (when FETCH was positive) compared with surrounding grids. As shown in Figure 3, most of these labeled grids are located in the western part of the study area and in the Himalayas, where the underlying surface is complicated.

Figure 4 shows the spatial pattern of the precipitation estimated by the FETCH_OCK model in August 2007. It can be observed that in the middle and eastern parts affected by the East Asian monsoon, the spatial pattern of FETCH_OCK is similar to OCK, because most of the values of FETCH in these regions are relatively low. This indicates that the underlying surface of these regions cannot disturb the spatial pattern of precipitation seriously. But in the western and

southern parts of the study area, the precipitation estimated by FETCH_OCK presents a seriously discontinuous surface compared with the result of OCK, because the spatial pattern of precipitation estimated by OCK was corrected by the extreme spatial variability of precipitation extracted from CMORPH satellite precipitation datasets. Furthermore, the ranges of the precipitation estimated by FETCH_OCK are closer to the rain gauge observation than are the ranges of OCK. Table 2 showed the maximum and minimum precipitation estimated by OCK and FETCH_OCK at the locations of the 133 rain gauges. The maximum precipitation values of OCK_DEM and FETCH_OCK were both underestimated, while the minimum values were overestimated. By comparison, the maximum and the minimum values of FETCH_OCK were closer to the range of rain gauge measurements than those of OCK_DEM in each month.

Validation and comparison with other precipitation datasets

In this section, the observations measured by independent rain gauges were used to validate the results of FETCH_OCK models. We first investigated whether FETCH_OCK shows obvious improvement in the input precipitation datasets (OCK and CMORPH). Performance

TABLE 2 Maximum and minimum values of OCK_DEM and FETCH_OCK at the locations of the 188 rain gauges.

Year	Month	Maximum (mm)			Minimum (mm)		
		Rain gauge	OCK_DEM	FETCH_OCK	Rain gauge	OCK_DEM	FETCH_OCK
2005	Jun	257.4	204.06	220.99	16.5	37.49	26.88
	Jul	529.0	254.01	292.23	40.4	72.75	78.45
	Aug	437.6	252.03	291.08	44.7	71.00	62.26
2006	Jun	232.6	235.46	222.01	24.8	48.93	29.29
	Jul	413.0	210.25	242.16	28.6	53.33	52.01
	Aug	236.5	263.44	190.78	22.7	57.68	32.81
2007	Jun	246.5	168.33	205.33	12.6	51.88	45.10
	Jul	314.8	283.52	310.28	48.1	70.15	59.76
	Aug	740.5	437.79	555.43	40.9	61.07	34.50
2008	Jun	230.3	190.40	215.71	29.4	56.44	51.27
	Jul	373.8	256.77	313.21	29.1	75.14	67.57
	Aug	379.0	240.52	306.46	39.6	59.55	35.83
2009	Jun	310.6	261.46	288.72	10.5	34.40	16.04
	Jul	558.2	326.95	305.78	25.9	56.51	44.27
	Aug	473.8	209.37	252.03	44.2	75.67	81.89

of FETCH_OCK was further assessed by comparing it with 2 widely used precipitation datasets: UK and TRMM 3B43.

Figure 5A–D show the R^2 , MAE, RMSE, and SSE, respectively, for summer precipitation (June to August) estimated by CMORPH, OCK, and FETCH_OCK between 2005 and 2009. It can be seen from Figure 5A that R^2 in the FETCH_OCK model was always above 0.5 and higher than in the other 2 precipitation datasets. In some months, the value of R^2 can reach up to 0.82, which indicates that the precipitation predicted by FETCH_OCK correlated well with the rain gauge observation. The RMSE of FETCH_OCK decreased to 26.76~66.77, compared with CMORPH (36.33~89.58) and OCK (29.22~70.56). The same decrease in MAE and SSE can be observed in Figure 5C and D. The 4 evaluation criteria indicated that FETCH_OCK presented substantial improvement in the precipitation estimate over the Tibetan Plateau when compared with OCK and CMORPH.

The R^2 , MAE, RMSE, and SSE, respectively, of FETCH, UK, and TRMM 3B43 are shown in Figure 6A–D. UK is an interpolation method that combines regression and kriging by treating these as 2 separate, consecutive steps. In this model, the secondary information is used to derive

the local mean of the primary attribute and then to perform simple kriging on the corresponding residuals (Brus and Heuvelink 2007). UK was used to estimate the precipitation, with elevation as a covariant, and showed better performance than other interpolation methods in many studies (Lloyd 2005; Bostan et al 2012). The unsampled point u was estimated by observations around u_i following Equation 13:

$$Z_{uk}(u) = a_0 + \sum_{k=1}^p a_k X_k(u) + \sum_{i=1}^n b_i \varepsilon(u_i) \quad (13)$$

where $Z_{uk}(u)$ is the prediction at location u , a_0 is the estimated intercept, a_k are the estimated regression model coefficients, $X_k(u)$ are the values of independent variables, b_i are the simple kriging weights derived from the spatial dependence structure of the residual, $\varepsilon(u_i)$ is the (observed) regression residual at location u_i , p is the number of the rain gauge observations, and n is the number of the observations around u .

It can be observed from Figure 6 that FETCH_OCK presented a higher value for R^2 , as well as lower RMSE, SSE, and MAE, than UK with DEM as a covariant in all months, which indicates that FETCH_OCK performed better than UK in estimating summer precipitation over

FIGURE 5 R^2 (A), MAE (B), RMSE (C), and SSE (D) of the summer precipitation (June to August) as estimated by CMORPH, OCK, and FETCH_OCK between 2005 and 2009.

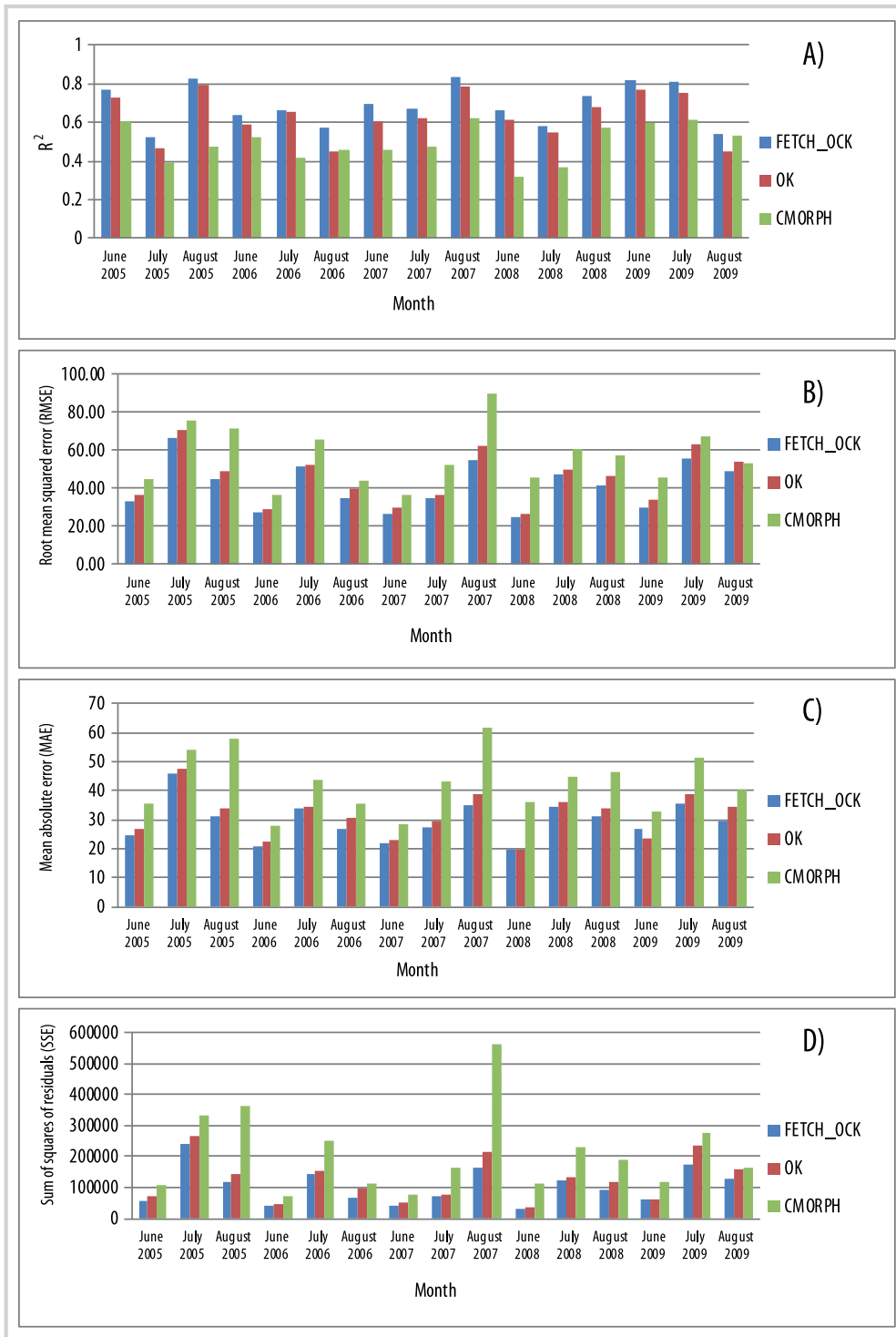
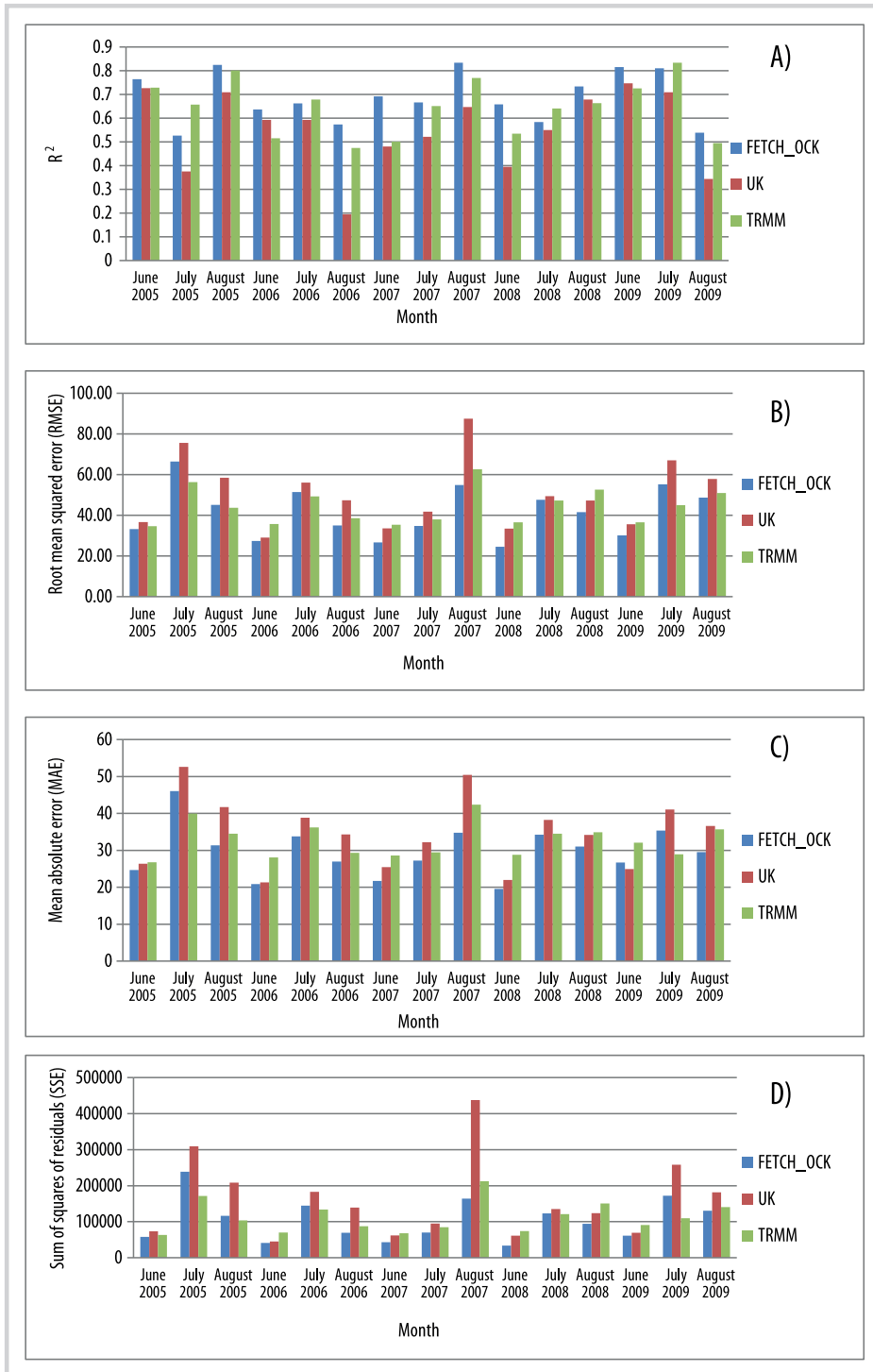


FIGURE 6 R^2 (A), MAE (B), RMSE (C), and SSE (D) of the summer precipitation (June to August) as estimated by the TRMM 3B43, UK, and FETCH_OCK models between 2005 and 2009.



the Tibetan Plateau. In comparison with TRMM 3B43, FETCH_OCK performed better in most months, except in July 2005 and 2009, when FETCH_OCK showed lower or similar R^2 and higher RMSE, SSE, and MAE. However,

even in these months, the R^2 of FETCH_OCK can reach as much as 0.53 (July 2005) and 0.81 (July 2009), which indicated that although the performance of FETCH_OCK is not as good as TRMM 3B43,

FETCH_OCK provided a reasonable spatial pattern of precipitation over the Tibetan Plateau in the 2 months.

Discussion

The Tibetan Plateau is a special region with the most complicated topography in the world, but the result of OCK with DEM as a covariant did not show the effect of topography. This problem was caused by the low correlation between DEM and rain gauge observations. Asli and Marcotte (1995) demonstrated that the covariant was worth introducing when the coefficient of determination was above 0.4. Goovaerts (2000) came to a similar conclusion, and later research showed that the result of kriging can be improved only when coefficients of determination between the primary data and the covariance are greater than 0.75. For all months in this study, the correlation between the rain gauge observations and DEM was very low (the R^2 in all months are between 0.1 and 0.3; data not shown here), so the introduction of topography into the geostatistical interpolation process cannot improve the smoothing effect.

As shown in Figure 3, the distribution of the labeled grids, which represents the locations with extreme small-scale spatial variability, is almost coincident with the distribution of lakes (which is labeled with a solid line in Figure 3) and the huge Himalaya mountains, which can cause extreme spatial variability of precipitation. So it can be inferred that the disturbance of the complicated underlying surface of the Tibetan Plateau by precipitation can be monitored by microwave remote sensing. By correcting the precipitation dataset estimated by OCK with FETCH derived from CMORPH, the spatial pattern of OCK substantially changed in the locations where the lakes and mountainous were distributed, and the results of the validation showed that the correction can improve the performance of OCK. This indicates that the smoothing effect is an important drawback of OCK and can lead to serious bias when it is used to simulate precipitation over mountainous regions. This drawback can be effectively corrected by the small-

scale spatial variability of precipitation derived from a microwave-based satellite precipitation dataset.

Conclusion

The rough terrain and the various types of land cover make the spatial distribution of precipitation over the Tibetan Plateau complicated. But precise estimation of the precipitation over this remote area is difficult because of the low density of the rain gauge network. In this study, a method based on geostatistical interpolation and remote sensing was proposed to estimate summer precipitation over the Tibetan Plateau. The main idea of this model is that the rain gauge observations are interpolated using OCK with DEM as a covariant, and the smoothing effect in the result of OCK is then corrected by the small-scale spatial variability of precipitation derived from the CMORPH satellite precipitation dataset. The summer precipitation (June to August) between 2005 and 2009 was estimated by FETCH_OCK using 133 rain gauge observations, and the results were validated by ground observations measured by 55 independent rain gauges. The performance of this model was further assessed by comparing it with the input datasets (OCK and CMORPH), as well as the precipitation estimated by UK and TRMM 3B43, which are widely used precipitation datasets. The results of the 4 criteria MAE, RMSE, R^2 , and SSE indicated that the precipitation dataset estimated by FETCH_OCK is not only more accurate than the input datasets but also superior to UK and TRMM 3B43 in most months. The method proposed in this study offers a new idea for correcting the smoothing effect inherent in all geostatistical-based interpolation methods when they are used to simulate precipitation.

A number of issues are worth further study. In particular, the precision of FETCH_OCK can only be validated in relatively rough spatial and temporal resolution (the spatial resolution is $0.25^\circ \times 0.25^\circ$, and the temporal resolution is monthly), so the applicability of this model on a smaller scale should be investigated. Meanwhile, we believe it would be meaningful to assess the performance of this model in other areas with low-density rain gauge networks.

ACKNOWLEDGMENTS

The rain gauge observations covering the Tibetan Plateau for this study were provided by the Institute of Tibetan Plateau Atmospheric and Environmental Science. The study had financial support from the Public Service Sectors (Meteorology) Special Fund Research (GYHY201006042), Major State Basic

Research Development Program of China (2013CB733405 and 2010CB950603), and National Natural Science Foundation of China (41201345).

REFERENCES

Akimov IV. 2004. Precipitation calculation method based on parameterization of distribution function evolution and its performance in global spectral atmospheric model. *Journal of Hydrology* 288(1–2):105–120.

Arkin PA, Meisner BN. 1987. The relationship between large-scale convective rainfall and cold cloud over the Western Hemisphere during 1982–84. *Monthly Weather Review* 115(1):51–74.

Asli M, Marcotte D. 1995. Comparison of approaches to spatial estimation in a bivariate context. *Mathematical Geology* 27(5):641–658.

Bostan PA, Heuvelink GBM, Akyurek SZ. 2012. Comparison of regression and kriging techniques for mapping the average annual precipitation of Turkey. *International Journal of Applied Earth Observation and Geoinformation* 19:115–126.

Brown JEM. 2006. An analysis of the performance of hybrid infrared and microwave satellite precipitation algorithms over India and adjacent regions. *Remote Sensing of Environment* 101(1):63–81.

- Brus DJ, Heuvelink GBM.** 2007. Optimization of sample patterns for universal kriging of environmental variables. *Geoderma* 138(1–2):86–95.
- Chinese Academy of Sciences, Computer Network Information Center.** 2013. International scientific and technical data mirror site. <http://datamirror.csdb.cn/index.jsp>; accessed on 17 March 2013.
- Condom T, Rau P, Espinoza JC.** 2011. Correction of TRMM 3B43 monthly precipitation data over the mountainous areas of Peru during the period 1998–2007. *Hydrological Processes* 25(12):1924–1933.
- Diodato N, Tartari G, Bellocchi G.** 2010. Geospatial rainfall modelling at eastern Nepalese highland from ground environmental data. *Water Resources Management* 24(11):2703–2720.
- Ferraro RR.** 1997. Special sensor microwave imager derived global rainfall estimates for climatological applications. *Journal of Geophysical Research* 102(D14):16715.
- Goovaerts P.** 1998. Ordinary cokriging revisited. *Mathematical Geology* 30(1):21–42.
- Goovaerts P.** 2000. Geostatistical approaches for incorporating elevation into the spatial interpolation of rainfall. *Journal of Hydrology* 228(1–2):113–129.
- Grimes DIF, Pardo-Iguzquiza E, Bonifacio R.** 1999. Optimal areal rainfall estimation using raingauges and satellite data. *Journal of Hydrology* 222(1–4):93–108.
- Grody NC.** 1984. Precipitation monitoring over land from satellites by microwave radiometry. In: Guyenne TD, Hunt JJ, editors. *Proceedings of the International Geoscience and Remote Sensing Symposium*. Noordwijk, the Netherlands: European Space Agency (EAS) Publications Division, pp 17–23.
- Grody NC.** 1991. Classification of snow cover and precipitation using the special sensor microwave imager. *Journal of Geophysical Research–Atmospheres* 96(D4):7423–7435.
- Gruber A, Su XJ, Kanamitsu M, Schemm J.** 2000. The comparison of two merged rain gauge–satellite precipitation datasets. *Bulletin of the American Meteorological Society* 81(11):2631–2644.
- Halle AT, Rientjes T, Gieske A, Gebremichael M.** 2010. Multispectral remote sensing for rainfall detection and estimation at the source of the Blue Nile River. *International Journal of Applied Earth Observation and Geoinformation* 12:S76–S82.
- Jia S, Zhu W, Lü A, Yan T.** 2011. A statistical spatial downscaling algorithm of TRMM precipitation based on NDVI and DEM in the Qaidam Basin of China. *Remote Sensing of Environment* 115(12):3069–3079.
- Joyce RJ, Janowiak JE, Arkin PA, Xie PP.** 2004. CMORPH: A method that produces global precipitation estimates from passive microwave and infrared data at high spatial and temporal resolution. *Journal of Hydrometeorology* 5(3):487–503.
- Karaseva MO, Prakash S, Gairola RM.** 2012. Validation of high-resolution TRMM 3B43 precipitation product using rain gauge measurements over Kyrgyzstan. *Theoretical and Applied Climatology* 108(1–2):147–157.
- Kebaili Bargaoui Z, Chebbi A.** 2009. Comparison of two kriging interpolation methods applied to spatiotemporal rainfall. *Journal of Hydrology* 365(1–2):56–73.
- Kidd C, Levizzani V.** 2011. Status of satellite precipitation retrievals. *Hydrology and Earth System Sciences* 15(4):1109–1116.
- Li M, Shao Q.** 2010. An improved statistical approach to merge satellite rainfall estimates and raingauge data. *Journal of Hydrology* 385(1–4):51–64.
- Lloyd CD.** 2005. Assessing the effect of integrating elevation data into the estimation of monthly precipitation in Great Britain. *Journal of Hydrology* 308(1–4):128–150.
- Michaelides S, Levizzani V, Anagnostou E, Bauer P, Kasparis T, Lane JE.** 2009. Precipitation: Measurement, remote sensing, climatology and modeling. *Atmospheric Research* 94(4):512–533.
- NASA [National Aeronautics and Space Administration].** 2013. Goddard Earth Sciences Data and Information Services Center: Mirador. <http://mirador.gsfc.nasa.gov/cgi-bin/mirador>; accessed on 12 March 2013.
- Olea RA, Pawlowsky V.** 1996. Compensating for estimation smoothing in kriging. *Mathematical Geology* 28(4):407–417.
- Rotstajn LD.** 1998. A physically based scheme for the treatment of stratiform clouds and precipitation in large-scale models. II: Comparison of modelled and observed climatological fields. *Quarterly Journal of the Royal Meteorological Society* 124(546):389–415.
- Shen MG, Tang YH, Chen J, Zhu XL, Zheng YH.** 2011. Influences of temperature and precipitation before the growing season on spring phenology in grasslands of the central and eastern Qinghai–Tibetan Plateau. *Agricultural and Forest Meteorology* 151(12):1711–1722.
- Sokol Z, Blížňák V.** 2009. Areal distribution and precipitation–altitude relationship of heavy short-term precipitation in the Czech Republic in the warm part of the year. *Atmospheric Research* 94(4):652–662.
- Tripoli GJ, Cotton WR.** 1980. A numerical investigation of several factors contributing to the observed variable intensity of deep convection over south Florida. *Journal of Applied Meteorology* 19(9):1037–1063.
- Turlapaty AC, Anantharaj VG, Younan NH, Joseph Turk F.** 2010. Precipitation data fusion using vector space transformation and artificial neural networks. *Pattern Recognition Letters* 31(10):1184–1200.
- Um M-J, Yun H, Jeong C-S, Heo J-H.** 2011. Factor analysis and multiple regression between topography and precipitation on Jeju Island, Korea. *Journal of Hydrology* 410(3–4):189–203.
- Villarini G, Krajewski WF.** 2008. Empirically based modeling of spatial sampling uncertainties associated with rainfall measurements by rain gauges. *Advances in Water Resources* 31(7):1015–1023.
- Ward E, Buytaert W, Peaver L, Wheeler H.** 2011. Evaluation of precipitation products over complex mountainous terrain: A water resources perspective. *Advances in Water Resources* 34(10):1222–1231.
- Wu C, Chen JM.** 2012. The use of precipitation intensity in estimating gross primary production in four northern grasslands. *Journal of Arid Environments* 82:11–18.
- Xie PP, Arkin PA.** 1996. Analyses of global monthly precipitation using gauge observations, satellite estimates, and numerical model predictions. *Journal of Climate* 9(4):840–858.
- Xie PP, Arkin PA.** 1997. Global precipitation: A 17-year monthly analysis based on gauge observations, satellite estimates, and numerical model outputs. *Bulletin of the American Meteorological Society* 78(11):2539–2558.
- Xie PP, Xiong AY.** 2011. A conceptual model for constructing high-resolution gauge–satellite merged precipitation analyses. *Journal of Geophysical Research–Atmospheres* 116.
- Yamamoto JK.** 2005. Correcting the smoothing effect of ordinary kriging estimates. *Mathematical Geology* 37(1):69–94.
- Yin Z-Y, Zhang X, Liu X, Colella M, Chen X.** 2008. An assessment of the biases of satellite rainfall estimates over the Tibetan Plateau and correction methods based on topographic analysis. *Journal of Hydrometeorology* 9(3):301–326.
- Zhao QY, Carr FH.** 1997. A prognostic cloud scheme for operational NWP models. *Monthly Weather Review* 125(8):1931–1953.